

Electronic Supplementary Information for New Journal of Chemistry

Construction of SAPO-34/SiO₂ composite: Effective catalyst for methanol to olefins reaction

Huiwen Huang^a, Shanshan He^a, Qiang Zhang^b, Wenyang Fan^a, Dongmei Xu^{a,*}, Jun Gao^a, Chunyi

Li^{b,*}

a. College of Chemical and Biological Engineering, Shandong University of Science and
Technology, Qingdao 266590, China

b. State Key Laboratory of Heavy Oil Processing, China University of Petroleum (East China),
Qingdao 266580, China

*Corresponding Author: xudongmei@sdust.edu.cn (D. Xu)

chyli_upc@126.com (C. Li)

S1. Experimental

S1.1. Chemicals

Commercial SAPO-34 zeolite ($\text{SiO}_2/\text{Al}_2\text{O}_3 = 0.4$, $\text{P}_2\text{O}_5/\text{Al}_2\text{O}_3 = 0.8$) was obtained from Catalyst Plant of Nankai University. Silica sol (SiO_2 , 30 wt%) was purchased from Qingdao Haiyang Chemical Co., China, phosphoric acid (H_3PO_4 , 85 wt%) and triethylamine (TEA, 99 wt%) were obtained from Sinopharm Chemical Reagent Co., China, pseudoboehmite (Al_2O_3 , 65 wt%) was bought from Aluminum Corporation of China.

S1.2. Characterizations

X-ray diffraction (XRD) patterns were collected by a D/Max RB diffractometer (Rigaku Co., Japan) with monochromatic Cu K α radiation (40 kV and 40 mA) in the 2 θ range from 5° to 65° at a scanning speed of 2 °/min.

The content of SAPO-34 zeolite in SAPO-34/SiO₂ composite was determined by comparing the integral intensity of the five characteristic diffraction peaks at 2 θ of 9.5°, 15.9°, 20.5°, 26.0° and 31.0° of SAPO-34/SiO₂ composite to that of an internal standard SAPO-34 sample (commercial SAPO-34 zeolite) using a working curve. The working curve was obtained by plotting the integral intensity of the aforementioned characteristic diffraction peaks versus the mass fraction of SAPO-34 zeolite in a series of mechanical mixtures of SAPO-34 and silica with the known mass fraction of SAPO-34.

Scanning electron microscope (SEM) images were obtained on an S-4800 field emission scanning electron microscopy (Hitachi Co., Japan) with an acceleration voltage of 3 kV.

Energy-dispersive X-ray spectroscopy (EDX) was conducted on an Sigma 300 field emission scanning electron microscopy (Zeiss Co., Germany) with a Smart EDX detector.

Nitrogen adsorption-desorption (N₂ adsorption-desorption) isotherms were measured by two Quadrasorb SI apparatus (Quantachrome, USA) at liquid nitrogen temperature (a mesopore analyzer for silica matrix and a micropore-mesopore analyzer for SAPO-34-based catalysts). Prior to the measurement, the silica matrix and catalyst sample were evacuated at 300 °C for 6 h to remove the adsorbed moisture. The total surface area was calculated by the Brunauer-Emmett-Teller (BET) equation and the total pore volume was estimated from the nitrogen adsorbed volume at relative pressure of 0.99. The micropore surface area and micropore volume of SAPO-

34-based catalysts were determined by the t-plot method. The external surface area and mesopore volume of SAPO-34-based catalysts were the difference between the total calculated value and the corresponding micropore data. The micropore and mesopore size distributions of silica matrix and SAPO-34-based catalysts were determined by the Barrett-Joyner-Halenda (BJH) method and Horvath-Kavazoe (HK) method, respectively.

Ammonia temperature programmed desorption (NH₃-TPD) profiles were examined on a TP-5079 adsorption instrument (Tianjin Xianquan Industrial and Trading Co., China) with an on-line thermal conductivity detector. Firstly, about 100 mg of catalyst sample of 80-180 mesh was loaded into a U-shaped microreactor and pretreated at 600 °C for 30 min with flowing argon (50 mL/min), and then cooled to 100 °C and saturated with ammonia. Secondly, the catalyst sample was purged with helium (30 mL/min) to remove the physically adsorbed ammonia until a stable TPD signal was attained. Finally, the temperature was increased from 100 °C to 600 °C at a constant heating rate of 10 °C/min.

Thermogravimetric (TG) curves were detected by a WCT-1D differential thermogravimetric analyzer (Beijing Beiguang Hongyuan Co., China). The catalyst sample was heated from 100 °C to 800 °C at a heating rate of 10 °C/min under flowing air (60 mL/min). The amount of the deposited coke on the catalyst sample after methanol conversion reaction was determined from the weight loss occurring at 400-700 °C from TG curves.

S1.3. Product analyses

The gaseous phase was analyzed on a Bruker 450 gas chromatography equipped with a HP-PLOT Al₂O₃ capillary column connected to a flame ionization detector, a 5A packed column connected to a thermal conductivity detector and a 5A packed column connected to a thermal

conductivity detector. The aqueous phase was analyzed on an Agilent 6820 gas chromatography equipped with a HP-INNOWAX capillary column connected to a flame ionization detector, using ethanol as the internal standard for calibration.

Methanol conversion was calculated by the difference between the inlet and outlet concentrations of methanol and dimethyl ether. Product selectivity on carbon basis was defined as the mass ratio of each product to all products. The mass balance was above 95 wt% for all catalyst evaluations in this study.

S1.4. Retained organics analysis

The retained organics in the catalyst samples after methanol conversion reaction were analyzed by gas chromatography-mass spectrometer (GC-MS). The catalyst sample was dissolved in a hydrofluoric acid solution (40 wt%), and the retained organics were extracted with dichloromethane and analyzed by an Agilent 7890B-GC equipped with an FID and a Agilent 5795C Mass Selective Detector with HP-5 capillary column. The structures annotated onto the chromatograms are peak identifications reference to NIST database. The amount of the retained organics was normalized with n-heptane as the internal standard.

Contents

Figures

Fig. S1 Flowchart of construction of SAPO-34/SiO₂ composite

Fig. S2 Flowchart of fabrication of SAPO-34-SiO₂ catalyst

Fig. S3 XRD pattern of silica matrix

Fig. S4 Working curve of mechanical mixtures of SAPO-34 and silica

Fig. S5 SEM images of SAPO-34/SiO₂ composite

Fig. S6 EDS results of SAPO-34/SiO₂ composite

Fig. S7 Micropore size distribution of SAPO-34/SiO₂ composite and mesopore size distribution of silica matrix

Fig. S8 NH₃-TPD profiles of SAPO-34 zeolite, SAPO-34-SiO₂ catalyst and SAPO-34/SiO₂ composite

Fig. S8 TG curves of SAPO-34 zeolite, SAPO-34-SiO₂ catalyst and SAPO-34/SiO₂ composite

Fig. S9 GC-MS analysis of retained organics in SAPO-34 zeolite and SAPO-34/SiO₂ composite after methanol conversion for 7 min

Tables

Table S1 Pore volume, surface area and pore diameter of SAPO-34/SiO₂ composite and silica matrix

Table S2 Reaction results of SAPO-34 zeolite, SAPO-34-SiO₂ catalyst and SAPO-34/SiO₂ composite in MTO reaction

Table S3 Conversion of methanol on SAPO-34 zeolite, SAPO-34-SiO₂ catalyst and SAPO-

34/SiO₂ composite with time on stream

Table S4 Pore volume and surface area of SAPO-34 zeolite and SAPO-34-SiO₂ catalyst

Table S5 Acid distribution of SAPO-34 zeolite and SAPO-34-SiO₂ catalyst

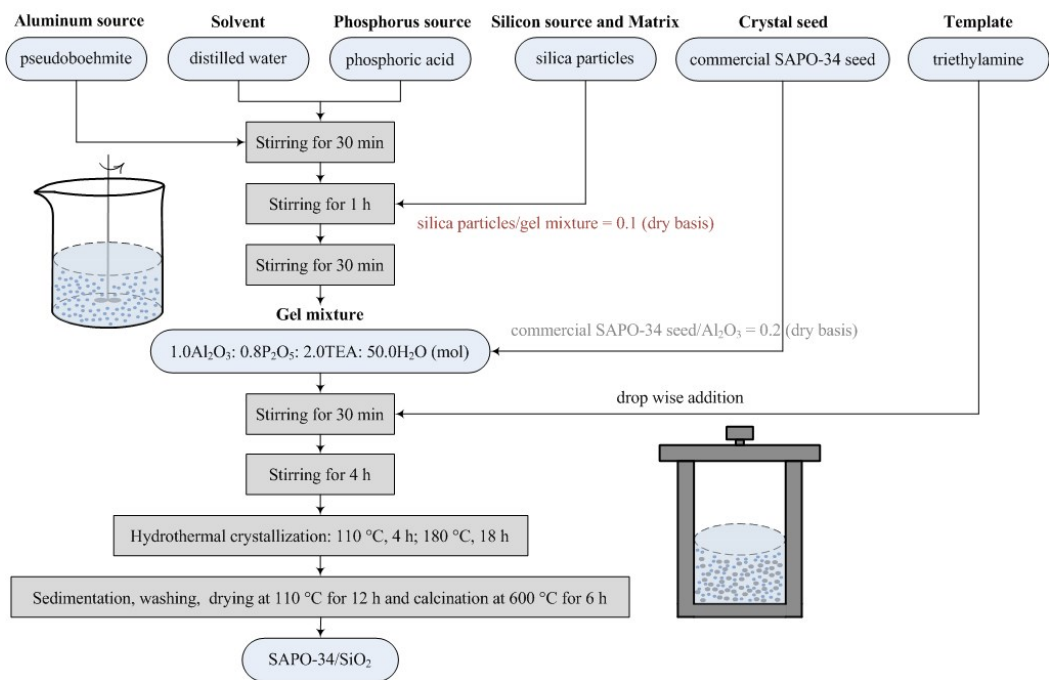


Fig. S1 Flowchart of construction of SAPO-34/SiO₂ composite

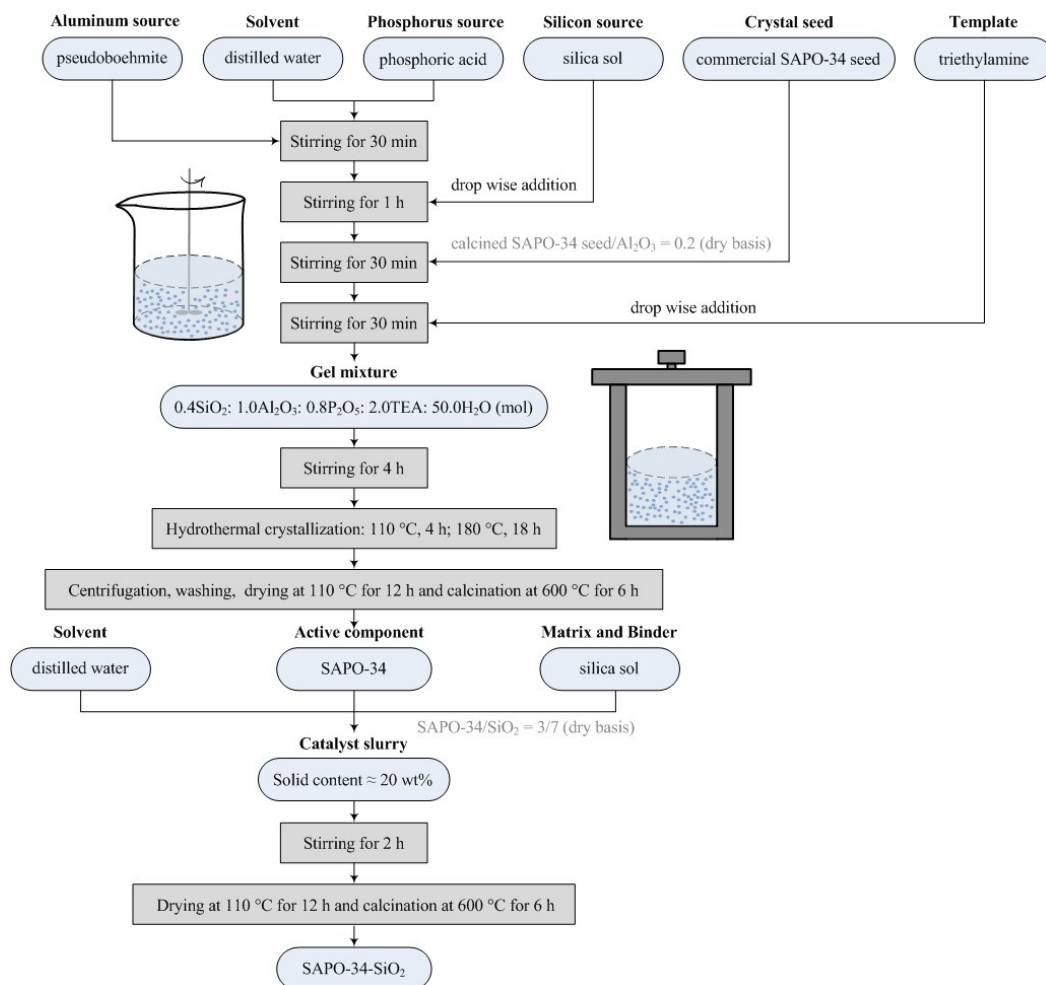


Fig. S2 Flowchart of fabrication of SAPO-34- SiO_2 catalyst

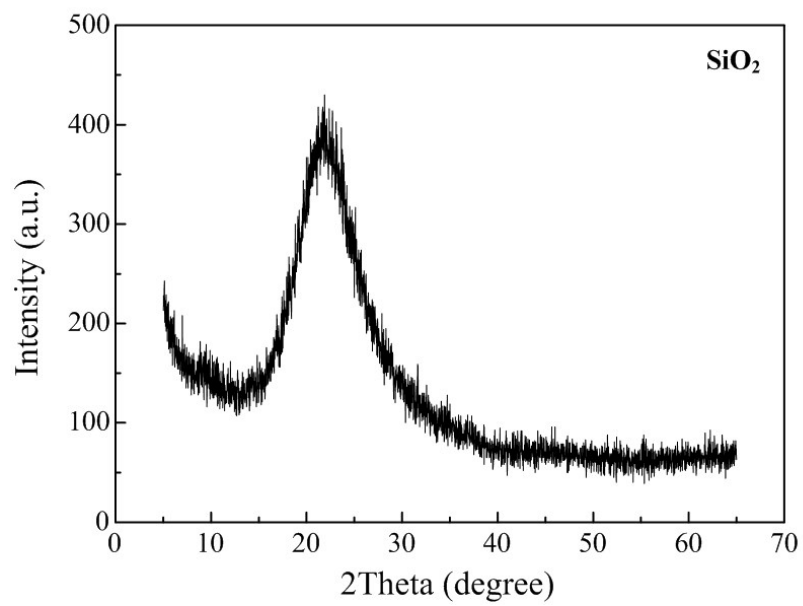


Fig. S3 XRD pattern of silica matrix

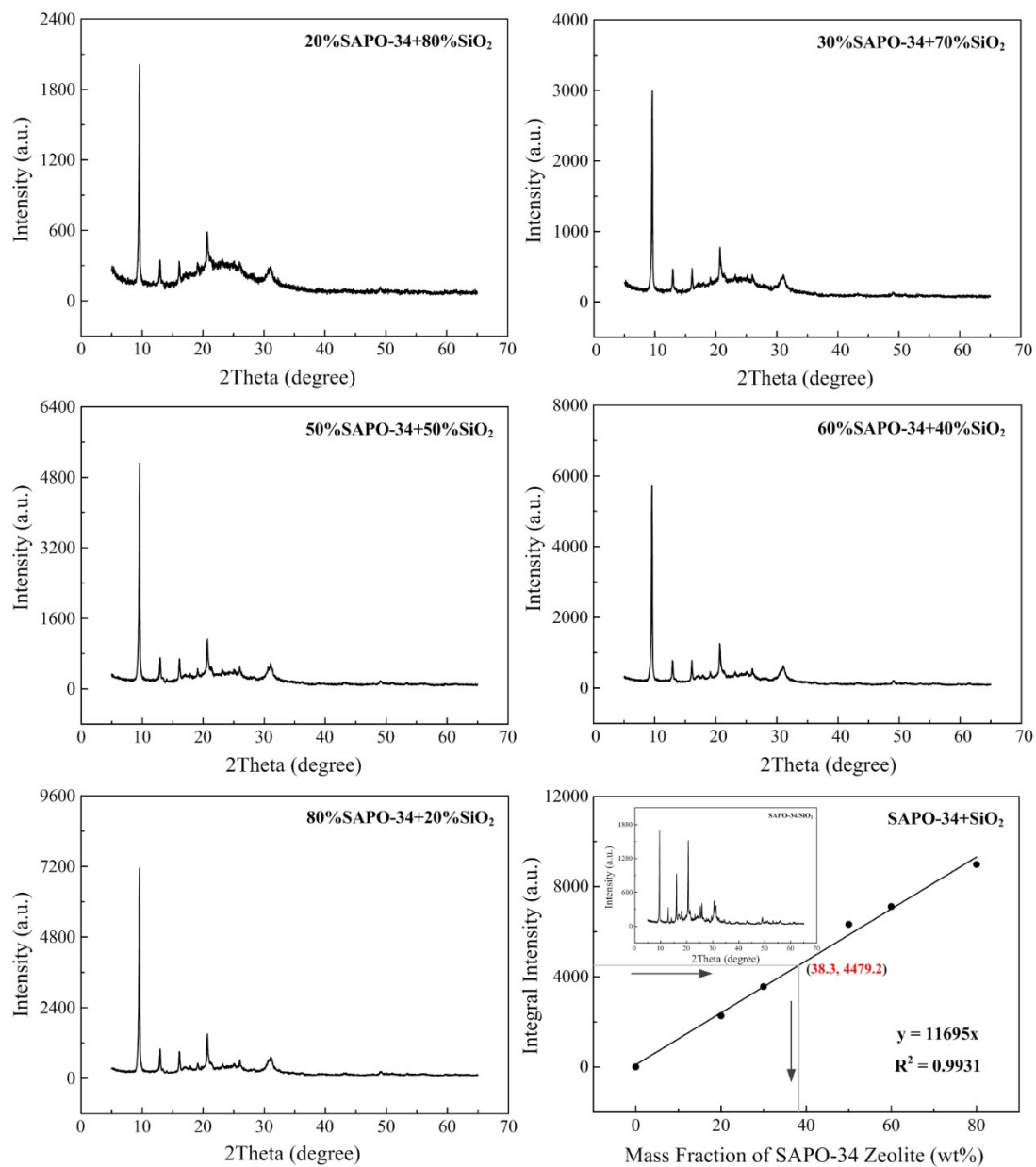


Fig. S4 Working curve of mechanical mixtures of SAPO-34 and silica

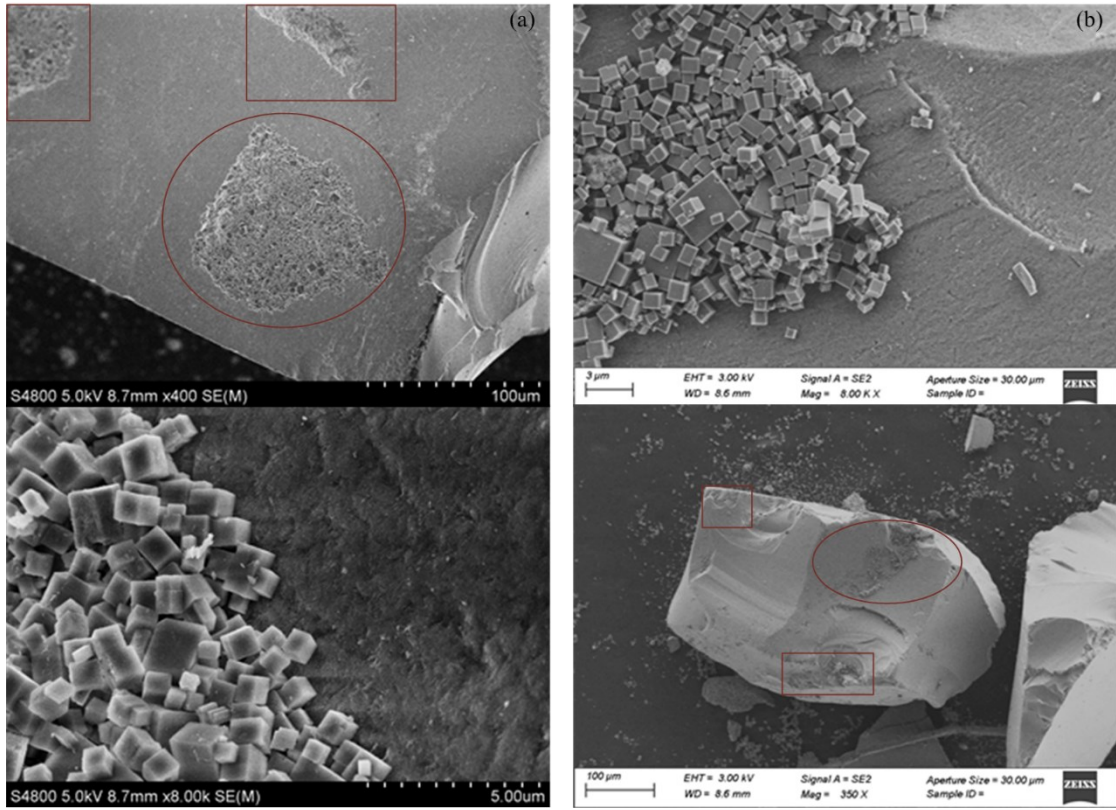
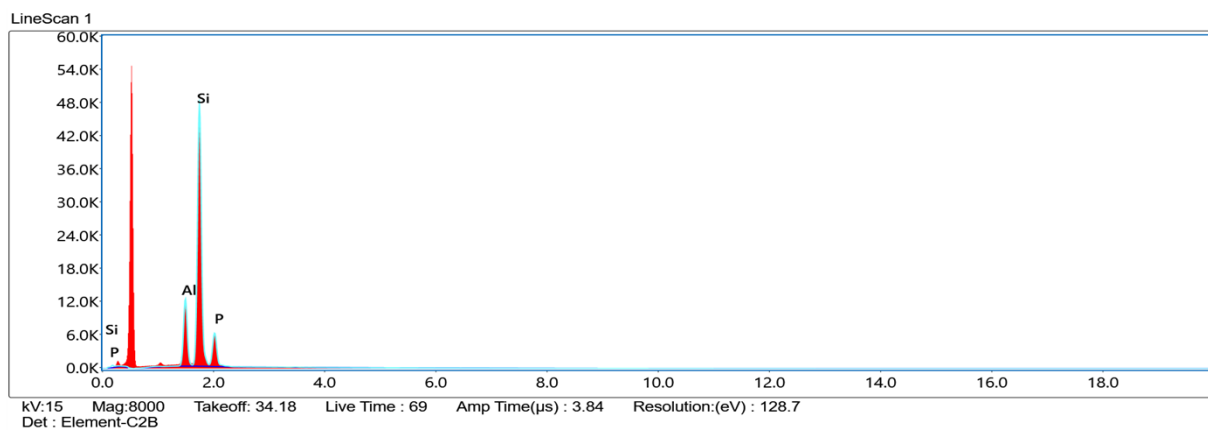
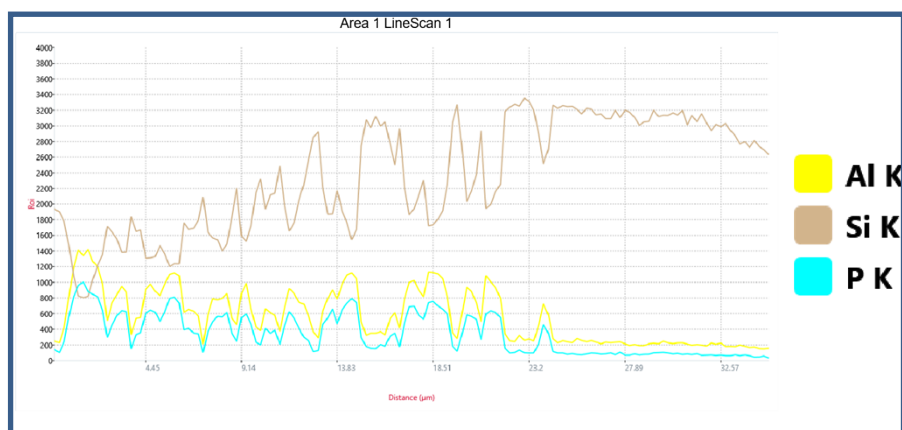
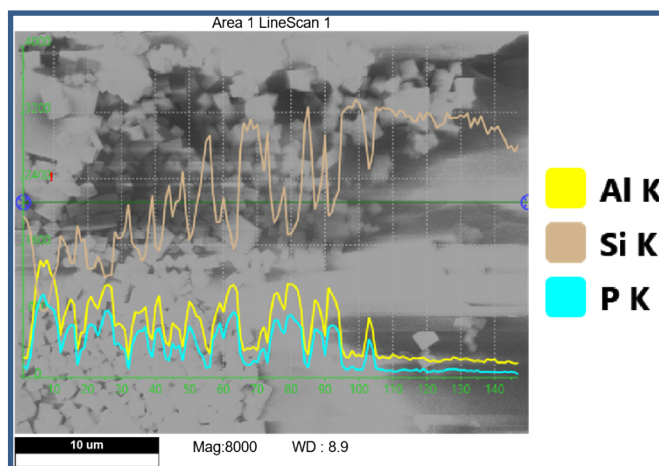


Fig. S5 SEM images of SAPO-34/SiO₂ composite

((a): Model: Hitachi S-4800 (b): Model: Zeiss sigma 300)



Element	Weight %	Atomic %	Error %	Net Int.	K Ratio	Z	A	F
Al K	14.69	15.46	2.11	1384.76	0.1413	0.9898	0.9612	1.0115
Si K	67.06	67.81	2.72	5709.88	0.5970	1.0105	0.8783	1.0032
P K	18.25	16.73	6.28	776.83	0.1042	0.9696	0.5888	1.0003

Fig. S6 EDS results of SAPO-34/SiO₂ composite (on the basis of the SEM images (Fig. S5(b)))

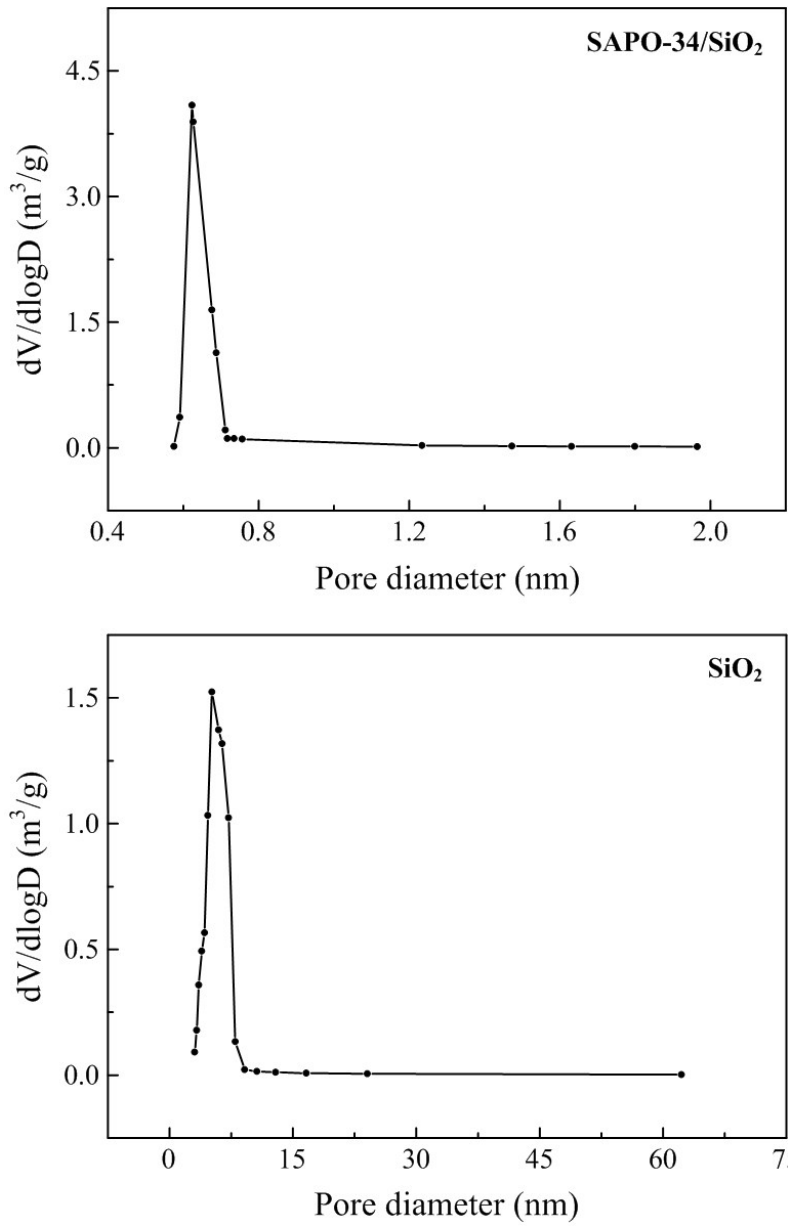


Fig. S7 Micropore size distribution of SAPO-34/SiO₂ composite and mesopore size distribution of silica matrix

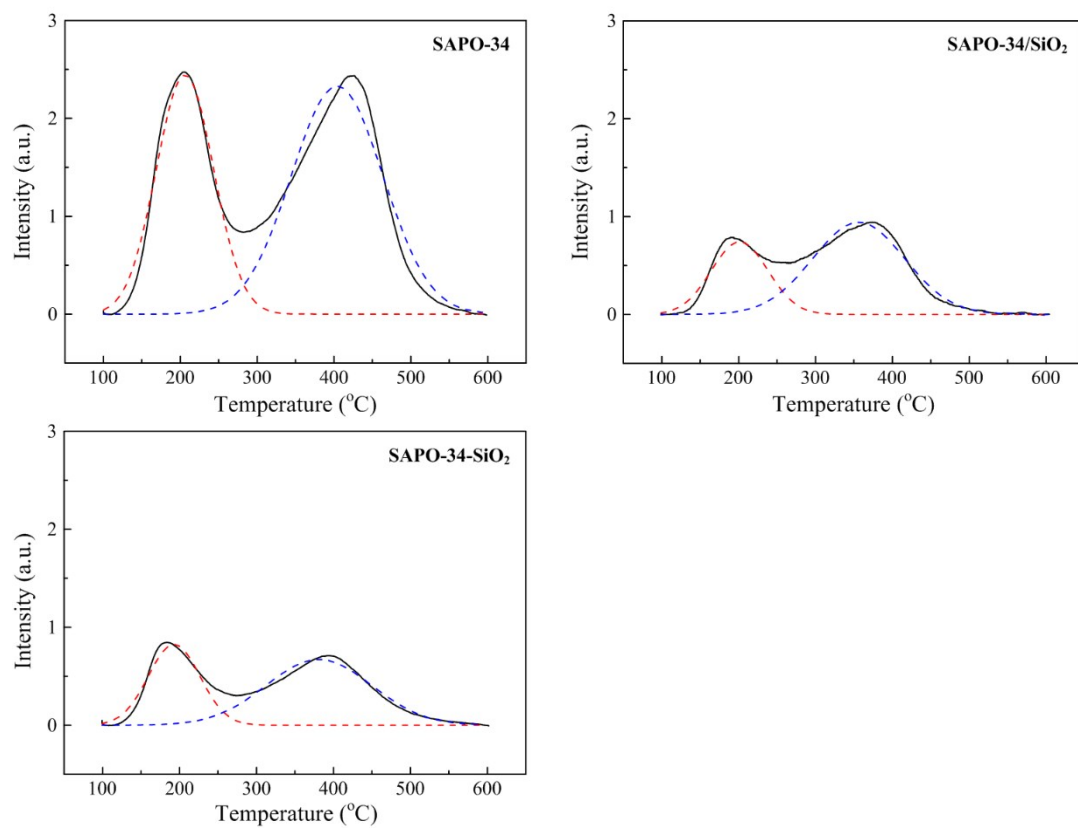


Fig. S8 NH₃-TPD profiles of SAPO-34 zeolite, SAPO-34-SiO₂ catalyst and SAPO-34/SiO₂ composite

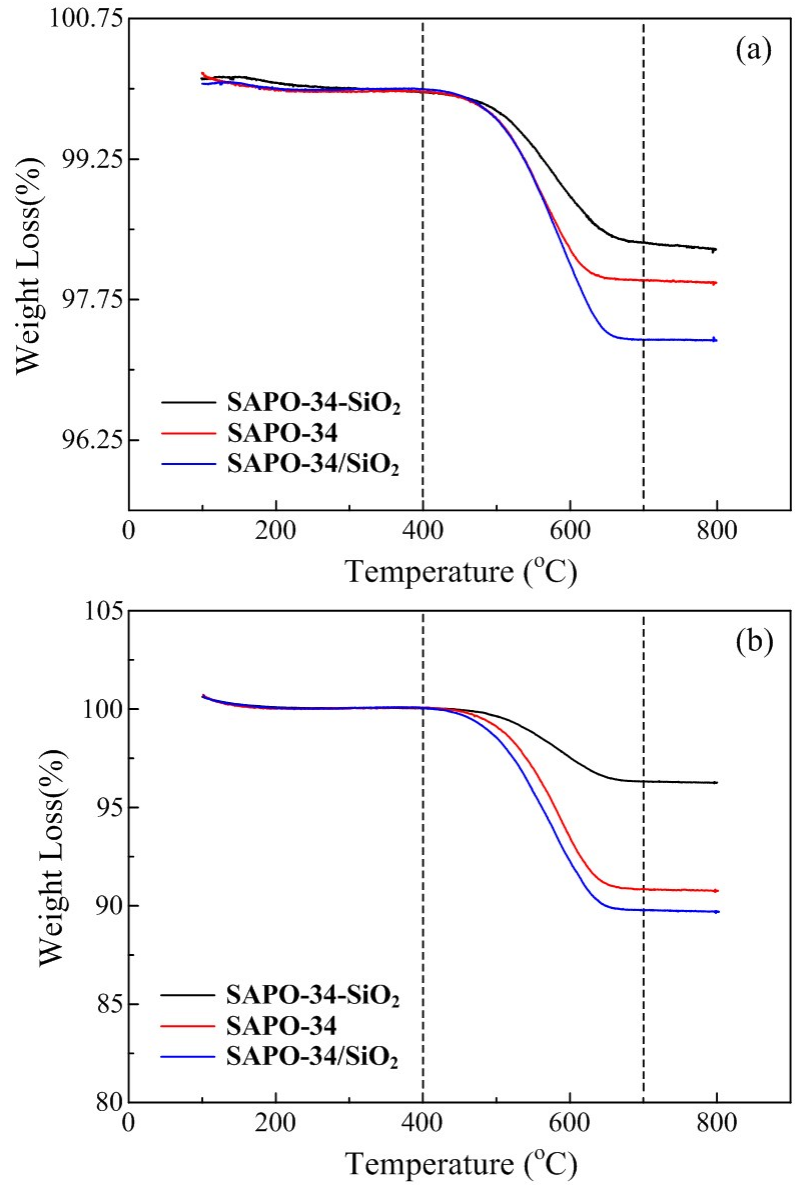


Fig. S9 TG curves of SAPO-34 zeolite, SAPO-34-SiO₂ catalyst and SAPO-34/SiO₂ composite

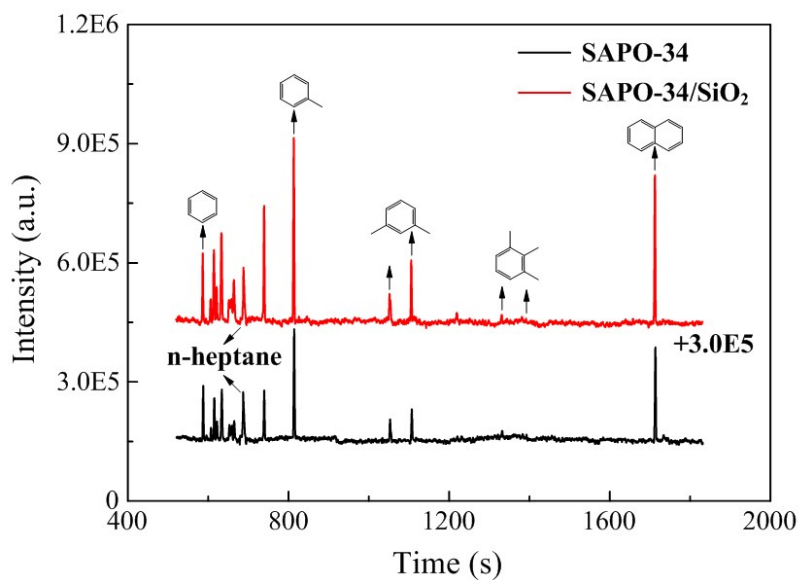


Fig. S10 GC-MS analysis of retained organics in SAPO-34 zeolite and SAPO-34/SiO₂ composite after methanol conversion for 7 min

Table S1 Pore volume, surface area and pore diameter of SAPO-34/SiO₂ composite and silica matrix

Sample	Pore volume (cm ³ /g)	Surface area (m ² /g)	Pore diameter (nm)	SAPO-34 content (wt%)
SAPO-34/SiO ₂	0.37	372.5	4.9	38.3 ^a /35.2 ^b
SiO ₂	0.37	273.1	5.1	-

a. Determined by the working curve.

b. Determined by the micropore surface area.

Table S2 Reaction results of SAPO-34 zeolite, SAPO-34-SiO₂ catalyst and SAPO-34/SiO₂ composite in MTO reaction

Sample	SAPO-34	SAPO-34-SiO ₂	SAPO-34/SiO ₂
Conversion (wt%)	99.98	99.94	99.96
Yield (C-wt%)			
H ₂	0.23	0.53	0.28
CO _x	0.18	1.00	0.55
CH ₄	3.11	4.19	4.71
C ₂ H ₆	1.05	2.03	0.87
C ₂ H ₄	44.17	47.39	55.18
C ₃ H ₈	3.95	3.90	1.68
C ₃ H ₆	38.14	34.13	31.37
C ₄ H ₁₀	0.35	0.27	0.14
C ₄ H ₈	8.05	6.10	5.18
C ₅ ⁺	0.76	0.41	-
C ₂ +C ₃	82.31	81.52	86.55
C ₂ -C ₄ ⁼	90.36	87.62	91.73
C ₂ ⁼ /C ₃ ⁼	1.16	1.39	1.76

Reaction conditions: T = 500 °C, WHSV = 9.78 h⁻¹.

Table S3 Conversion of methanol on SAPO-34 zeolite, SAPO-34-SiO₂ catalyst and SAPO-34/SiO₂ composite with time on stream in MTO reaction

Time on stream (min)	Conversion (wt%)		
	SAPO-34	SAPO-34-SiO ₂	SAPO-34/SiO ₂
0-5	99.93	99.13	99.08
20-25	99.94	88.23	99.90
40-45	99.92	79.21	99.83
60-65	99.55	-	99.41
80-85	99.02	-	99.06
100-105	87.75	-	90.70

Reaction conditions: T = 500 °C, MeOH : H₂O = 1 : 4 (mol), WHSV = 3.36 h⁻¹.

Table S4 Pore volume and surface area of SAPO-34 zeolite and SAPO-34-SiO₂ catalyst

Sample	Pore volume (cm ³ /g)			Surface area (m ² /g)		
	V _{Mirco}	V _{Meso}	V _{Total}	S _{Mirco}	S _{Ext}	S _{Total}
SAPO-34	0.25	0.05	0.30	735.8	3.1	738.9
SAPO-34-SiO ₂	0.03	0.33	0.36	67.0	207.3	274.3

Table S5 Acid distribution of SAPO-34 zeolite and SAPO-34-SiO₂ catalyst

Sample	Acid distribution (mmol/g)		
	Total	Strong	Weak
SAPO-34	0.91	0.55	0.36
SAPO-34-SiO ₂	0.29	0.18	0.11